Global Change Biology
celebrating 20 years

Global Change Biology (2014), doi: 10.1111/gcb.12681

A global assessment of forest surface albedo and its relationships with climate and atmospheric nitrogen deposition

STEFANO LEONARDI[1], FEDERICO MAGNANI[2], ANGELO NOLÈ[3], TWAN VAN NOIJE[4] and MARCO BORGHETTI[3]

[1]*Dipartimento di Bioscienze, Università di Parma, Parma, Italy,* [2]*Dipartimento di Scienze Agrarie, Università di Bologna, Bologna, Italy,* [3]*Scuola di Scienze Agrarie, Forestali, Alimentari e dell'Ambiente, Università della Basilicata, Potenza, Italy,* [4]*Royal Netherlands Meteorological Institute (KNMI), De Bilt, The Netherlands*

Abstract

We present a global assessment of the relationships between the short-wave surface albedo of forests, derived from the MODIS satellite instrument product at 0.5° spatial resolution, with simulated atmospheric nitrogen deposition rates (N_{dep}), and climatic variables (mean annual temperature T_m and total annual precipitation P), compiled at the same spatial resolution. The analysis was performed on the following five forest plant functional types (PFTs): evergreen needle-leaf forests (ENF); evergreen broad-leaf forests (EBF); deciduous needle-leaf forests (DNF); deciduous broad-leaf forests (DBF); and mixed-forests (MF). Generalized additive models (GAMs) were applied in the exploratory analysis to assess the functional nature of short-wave surface albedo relations to environmental variables. The analysis showed evident correlations of albedo with environmental predictors when data were pooled across PFTs: T_m and N_{dep} displayed a positive relationship with forest albedo, while a negative relationship was detected with P. These correlations are primarily due to surface albedo differences between conifer and broad-leaf species, and different species geographical distributions. However, the analysis performed within individual PFTs, strengthened by attempts to select 'pure' pixels in terms of species composition, showed significant correlations with annual precipitation and nitrogen deposition, pointing toward the potential effect of environmental variables on forest surface albedo at the ecosystem level. Overall, our global assessment emphasizes the importance of elucidating the ecological mechanisms that link environmental conditions and forest canopy properties for an improved parameterization of surface albedo in climate models.

Keywords: albedo, climate, forest, MODIS, nitrogen deposition

Received 2 April 2014; revised version received 29 May 2014 and accepted 28 June 2014

Introduction

Land surface albedo, the ratio of reflected to incident shortwave (SW) solar radiation at the surface over land, is an important factor that drives the Earth's radiation budget and influences the exchange of heat and matter between the land surface and the atmosphere. This implies relevant bio-geophysical feedbacks between the land surface albedo and the climate system, so that inaccuracies in the specifications of surface albedo parameters might translate into major errors in global climate models (Dickinson, 1983).

Surface albedo is considerably lower for vegetation than for bare soil and snow. Surface albedo also depends on vegetation type and is lower for forests compared to other vegetation biomes like grasslands and pastures. This is derived from different types of observations, for example from remotely sensed global maps of land surface albedos produced by the MODIS (Moderate Resolution Imaging Spectroradiometer) sensor carried on the Terra and Aqua satellites (Schaaf *et al.*, 2002; Gao *et al.*, 2005), from direct measurements of surface albedo changes following afforestation of soil or pastures (Kirschbaum *et al.*, 2011) and during vegetation succession after the occurrence of fire (McMillan & Goulden, 2008).

Forests cover about 30% of the land surface, therefore expansion of forests as a consequence of global warming may represent a relevant positive climate feedback (Bonan, 2008) as inferred, for instance, from past climatic changes, *e.g.* during the warming of the mid-Holocene (6000 years BP) (Gallimore *et al.*, 2005). The evergreen needle-leaf boreal forest, in particular, has the lowest surface albedo, and therefore the greatest potential bio-geophysical effect on climate warming (Betts & Ball, 1997; Betts, 2000).

Correspondence: Marco Borghetti, Scuola di Scienze Agrarie, Forestali, Alimentari e dell'Ambiente, Università della Basilicata, viale dell'Ateneo Lucano 10, Potenza 85100, Italy, tel. +39 0971 205246, fax +39 0971 205376, e-mail: marco.borghetti@sisef.org

Forest surface albedo is spatially variable and temporally dynamic, with a number of environmental variables having a strong influence on plant and canopy traits associated with surface reflectivity, including forest composition, i.e. abundance of broad-leaf vs. needle-leaf species, leaf area index (LAI), leaf morphology, crown geometry, and leaf area distribution, among other attributes (Ollinger, 2011). Many of these traits might undergo strong environmental control, and can be affected by changes in climatic and atmospheric conditions, both locally and globally.

The anthropogenic perturbation of the nitrogen cycle, caused by fossil fuel combustion and agricultural emissions, is an important driver of environmental changes at local and global scales (Ciais *et al*., 2013): an impressive amount ($\sim 18 \times 10^6$ kg) of reactive nitrogen is being deposited into forests each year (Gruber & Galloway, 2008; Schlesinger, 2009), with relevant effects on forest carbon cycle (Magnani *et al*., 2007; Guerrieri *et al*., 2010; Thomas *et al*., 2010). Nitrogen deposition can also modify leaf nutritional status and leaf structure by both increased nitrogen plant uptake and direct canopy retention, which is reported to reach 70% of the atmospheric nitrogen deposition (Gaige *et al*., 2007; Sievering *et al*., 2007; Dail *et al*., 2009). As an example of the effect on leaf and canopy properties, Leonardi *et al*. (2012) recently reported an association between annual nitrogen deposition rate and intrinsic leaf water use efficiency for a range of angiosperm and conifer forest tree species.

The relationship between nitrogen concentration in forest canopies and surface albedo has been intensively debated in recent years. Ollinger *et al*. (2008) reported a high positive correlation between foliar nitrogen concentration and vegetation canopy bidirectional reflectance distribution function (BRDF) in the near infrared (NIR) spectral region at peak growing season in North America temperate and boreal forests from MODIS images, suggesting the possibility of a negative feedback in the climate system due to the nitrogen cycle. However, in a subsequent study, Knyazikhin *et al*. (2012) indicated the correlation was a consequence of variability in forest structure and composition (differences in canopy geometry primarily due to differences between conifer and broad-leaf species) rather than leaf nitrogen concentration. Therefore, a debate has arisen focused on the following points: (i) surface albedo (both NIR and SW broadband albedo) from satellite data cannot be directly related to leaf level processes, rather it is primarily determined by canopy architectural properties; and (ii) regardless of leaf structural properties, canopy architecture and reflectivity co-vary among forest functional types (Townsend *et al*., 2013), suggesting underlying ecological drivers of canopy albedo.

Therefore, effects of altered nitrogen cycling and soil nitrogen availability that result from atmospheric nitrogen deposition (Aber *et al*., 2003; Phoenix *et al*., 2012) on multiple plant and canopy traits potentially affecting surface albedo (Ollinger, 2011) cannot be ruled out. For example, increased nitrogen mineralization and availability rates might drive differential plant carbon allocation (*e.g.* Albaugh *et al*., 1998; Gower *et al*., 1992), hence a different canopy structure; as site fertility increases, stand density might decline (Westoby, 1984), with an effect on canopy geometry. In the long-term, forest composition can also be affected by altered nutrient availability (Zaccherio & Finzi, 2007; Bobbink *et al*., 2010), with the resulting effect on surface albedo due to differences in crown reflectivity properties, e.g. between conifer and hardwood species.

A suite of standard albedo products have been provided by the MODIS satellite instrument (Schaaf *et al*., 2002), therefore land surface albedo variability, its dependence on vegetation type, vegetation and land-use changes, as well as its relevance for modeling land surface processes have been extensively explored in recent years (*e.g*. Zhou *et al*., 2003; Barnes & Roy, 2010; Jin *et al*., 2011). MODIS albedo has also been successfully compared with *in situ* albedo measurements at a number of forest sites (Cescatti *et al*., 2012).

However, a global assessment of the relationship between forest surface albedo and environmental conditions remains unavailable. Here, for the purposes of pattern interpretation, and as an attempt to define possible links between environmental conditions and forest canopy properties, we have globally explored the relationships between forest surface short-wave albedo, as derived from the satellite MODIS instrument, simulated atmospheric nitrogen deposition, mean annual temperature, and total annual precipitation.

Materials and methods

Land surface albedo and land classification map

The land surface albedo data set analyzed in this study was derived from the statistical product at 0.5° spatial resolution generated from the MODIS BRDF (MOD43B3, 16-Day L3 Global 1 km SIN Grid) filled-land surface albedo map product. The following file: AlbBoxStats.ET.HD.00-04.WS.c004.v2.0.tar.gz was retrieved on 24 October 2013 from: ftp://modisatmos.gsfc.nasa.gov/L3LandSurfaceProducts/Data/Albedo/Statistics/FilledMapsByEcoType/AlbBoxStats.FilledMapsByEcoType.0004.c004.v2.0/WhiteSky/ByResolution.WS.c004.v2.0/.

This file contains spatially continuous 5 year aggregated (5 year mean) albedo climatology obtained by screening 5 years (2000, 2001, 2002, 2003 and 2004) of MOD43B3 albedo data to remove lower quality and snow-covered pixels, and to fill gaps (Fang *et al*., 2007). White-sky

albedos, *i.e.* albedos produced under diffuse illumination conditions (isotropic incident radiation), which should not be affected by latitude *per se* (Schaaf *et al*., 2002), are provided for seven spectral bands (MODIS channels 1–7) and three broad-bands (0.3–0.7 μm, 0.7–3.0 μm, and 0.3–5.0 μm).

For each 0.5° geographic pixel of each wavelength for each of 23 sixteen-day periods per year (001, 017, 033,...353), albedo statistics (mean, standard deviation, and pixel counts, computed from 1 min spatial resolution product; see http://modis-atmos.gsfc.nasa.gov/ALBEDO/index.html) were provided for 17 IGBP plant functional types (PFTs) (Loveland & Belward, 1997).

We selected white-sky albedos for the spectral band 0.3–5 μm attributed to the following PFTs: (i) evergreen needle-leaf forests (ENF, lands dominated by needle-leaf woody vegetation with a percent cover >60% and height exceeding 2 m, almost all trees remain green all year, canopy is never without green foliage); (ii) evergreen broad-leaf forests (EBF, lands dominated by broadleaf woody vegetation with a percent cover >60% and height exceeding 2 m, almost all trees and shrubs remain green year-round, canopy is never without green foliage); (iii) deciduous needle-leaf forests (DNF, lands dominated by woody vegetation with a percent cover >60% and height exceeding 2 m, consists of seasonal needle-leaf tree communities with an annual cycle of leaf-on and leaf-off periods); (iv) deciduous broad-leaf forests (DBF, lands dominated by woody vegetation with a percent cover >60% and height exceeding 2 m, consists of broadleaf tree communities with an annual cycle of leaf-on and leaf-off periods); and (v) mixed-forests (MF, lands dominated by trees with a percent cover >60% and height exceeding 2 m, consists of three communities with interspersed mixtures or mosaics of the other four forest types) (Loveland & Belward, 1997; Friedl *et al*., 2002). The area covered by these PFTs corresponds to 20% of total continental land surface (ENF 4.2%, EBF 10.4%, DNF 1.4%, DBF 1.2% and MF 4.9%) and to 35.4% of land surfaces covered by IGBP vegetation classes 1–11.

We used the IGBP land ecosystem classification map available at one-minute spatial resolution (see http://modisatmos.gsfc.nasa.gov/ECOSYSTEM/index.html). The following file: IGBP.EcoMap.v1.0.2004.129.v004.hdf.gz was retrieved on 24 October 2013 from: ftp://modis-atmos.gsfc.nasa.gov/L3LandSurfaceProducts/Data/Ecosystem/.

We successively averaged data over four sixteen-day periods (i.e. averaged periods starting at days 1, 17, 33, 49 from approximately January–February for the southern hemisphere; and averaged periods starting at days 177, 193, 209 and 225, from approximately July–August for the northern hemisphere), which corresponded to snow-free periods at peak growing season in each hemisphere.

Normalized difference vegetation index

Normalized difference vegetation index (*NDVI*) is one of the most extensively applied vegetation indices related to *LAI* (Myneni *et al*., 1995). We used the spatially continuous 5 year (2000–2004) aggregated *NDVI* map available at 1-min spatial resolution on a 16-day basis per year, calculated from MODIS bands 1 and 2 of the spatially complete white-sky albedo maps (see http://modis-atmos.gsfc.nasa.gov/NDVI/index.html).

The following file: NDVI.00-04.c004.v2.0.tar.gz was retrieved on October 24 2013 from: ftp://modis-atmos.gsfc.nasa.gov/L3LandSurfaceProducts/Data/NDVI/Maps/. *NDVI* were binned to a PFTs map, and averages for the same four sixteen-days (see above) were calculated. *NDVI* values at 1 min spatial resolutions were successively averaged over each 0.5° geographic pixel, for each PFT.

Climatic variables and nitrogen atmospheric deposition

For each of the same 0.5° geographic pixels, annual climatic variables (mean annual temperature T_m and total annual precipitation P) were extracted from the 0.5° × 0.5° CRU TS 2.1 global climatic gridded dataset available for download from the Climatic Research Unit of University of East Anglia, Norwich, UK (http://www.cru.uea.ac.uk/cru/data/hrg/), and averaged from 1970 to 2006.

For each of the same 0.5° resolution pixels, mean annual total atmospheric reactive nitrogen deposition (N_{dep}) from 1960 to 2004 was estimated from a TM4 chemistry-transport model simulation (Schultz *et al*., 2007). Total reactive N includes oxidized reactive components (NO_y, also including peroxyacyl nitrates and organic nitrates), and reduced reactive compounds (NH_x, including both ammonia NH_3 and ammonium NH_4). The simulation was carried out at a horizontal resolution of 3° (longitude) × 2° (latitude) and the results were successively interpolated to a 0.5° × 0.5° grid, as described in Leonardi *et al*. (2012).

Compiled data sets

Two data sets were analyzed. *Data set one*. For each 0.5° resolution pixel, we used surface albedo means attributed to the following PFTs: ENF, EBF, DBF, DNF, and MF; for each PFT, we used only pixels in which pixel count (i.e. the number of 1-min spatial resolution contributing pixels) was ≥10. *Data set two*. In an attempt to restrict the analysis on 'pure' PFT pixels, we assumed that in a geographic region where a single PFT is dominant, the probability is lower of small-scale variability in forest composition, e.g. different mixtures of broad-leaf and needle-leaf canopy trees, that were not detected by satellite measurements; in doing so, we assumed a positive correlation between within-pixel and among-pixels variability. Thus, from data set one, a second data set was generated using the following procedure: for each 0.5° pixel, a 'heterogeneity' index (H) was calculated as $H = 1 - \sum p_i^2$, where p_i is the frequency of each PFT in the 0.5° resolution pixel, based on pixel counts associated with each PFT in the original data set (see above). Successively, for a given PFT, we selected only 0.5° geographic pixels where $H < 0.1$ and $p_i > 0.5$; this implies that in such pixels more than 90% of sub-pixels are classified with identical PFT.

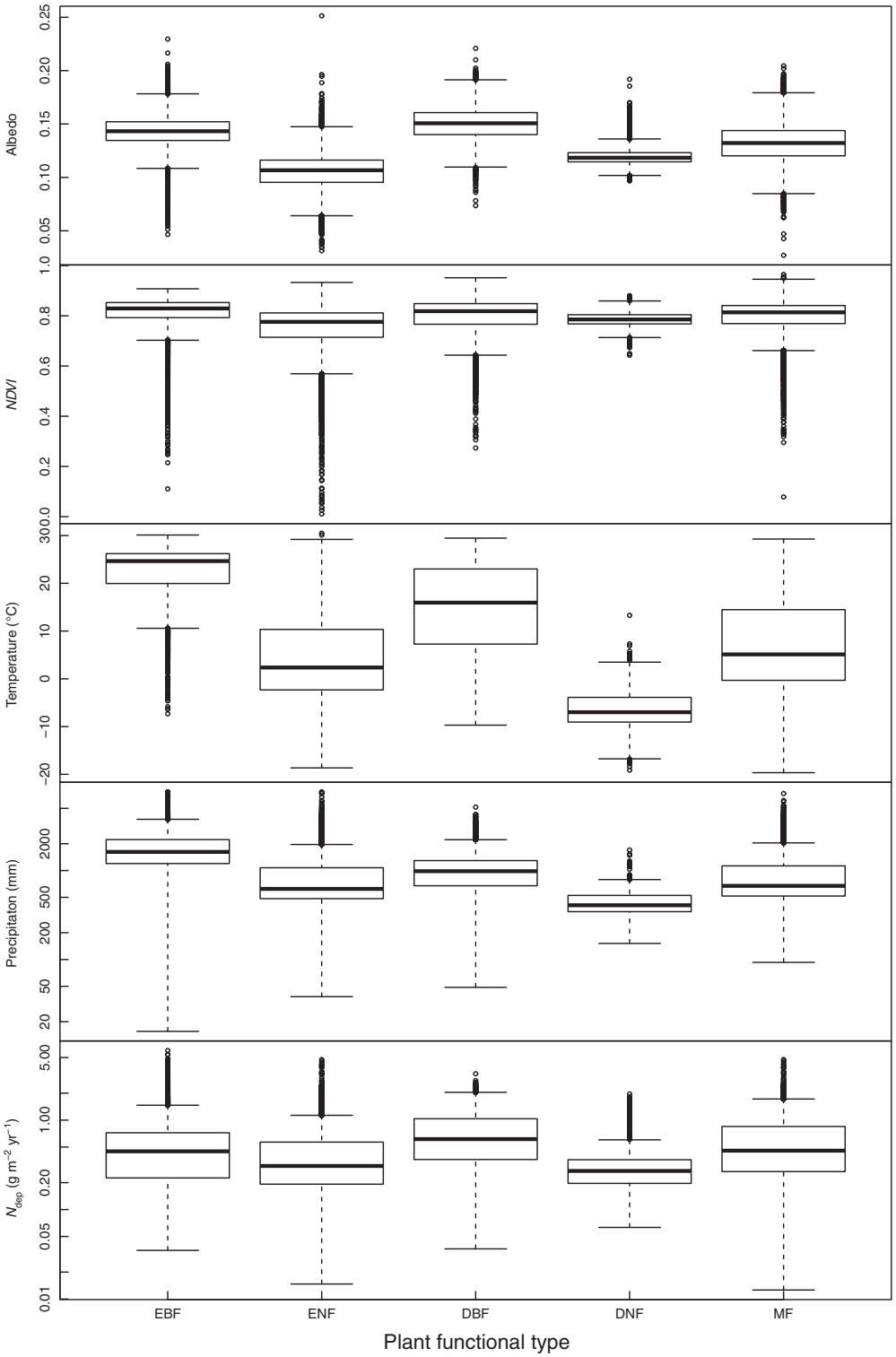

Fig. 1 Albedo boxplot, Normalized Differential Vegetation Index (*NDVI*), mean annual temperature, total annual precipitation, and mean annual atmospheric nitrogen deposition rate (N_{dep}) for different plant functional types (evergreen broad-leaf forests (EBF); evergreen needle-leaf forests (ENF); deciduous broad-leaf forests (DBF); deciduous needle-leaf forests (DNF); mixed-forests (MF)) in *data set one*; the box represents from the 75th percentile to the 25th percentile, and the line inside the median; upper and lower marks are the largest (smallest) observation values that are less than or equal to the upper (lower) quartile plus 1.5 the length of the interquartile range; circles outside the lower-upper mark range are outliers.

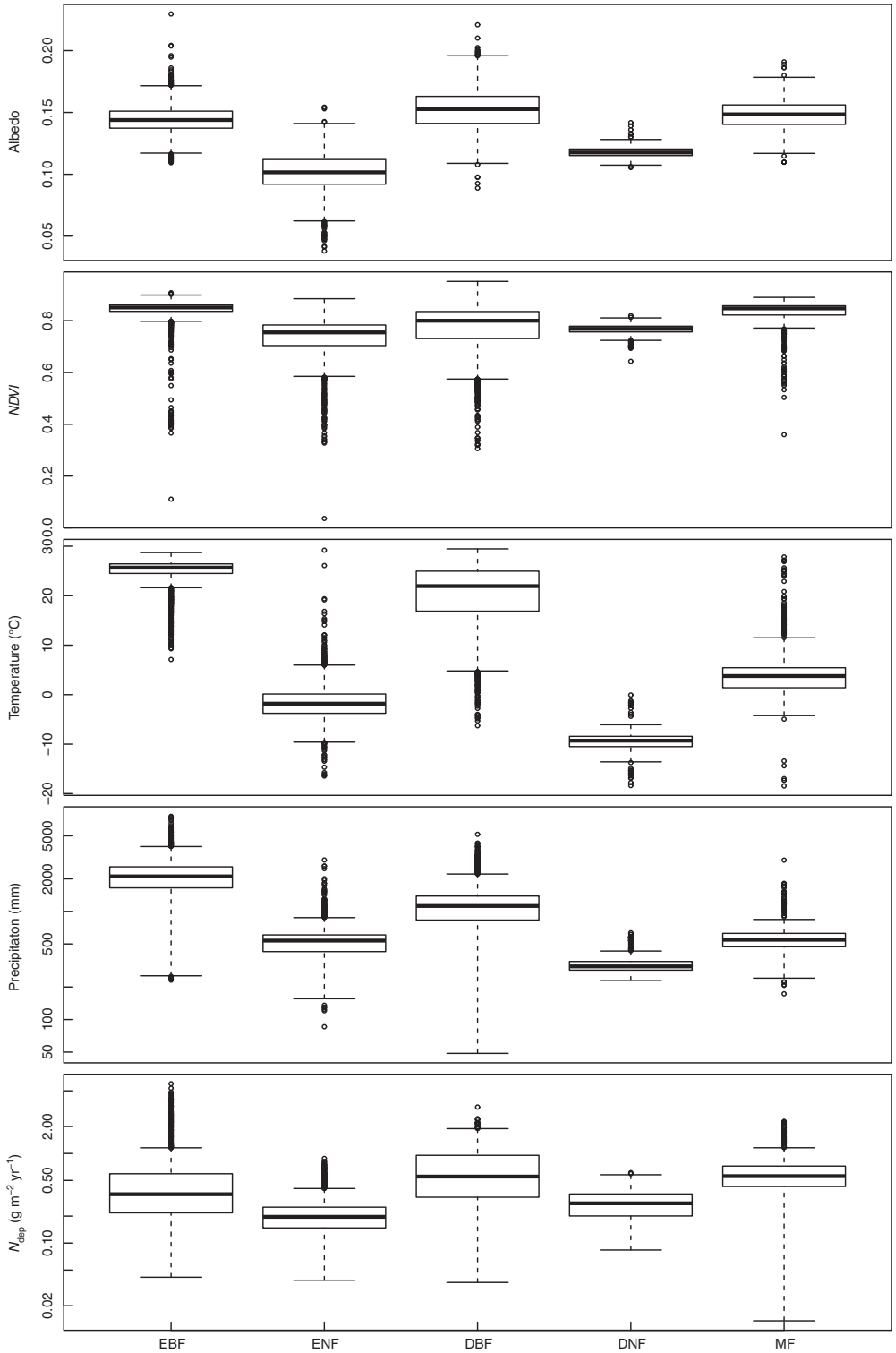

Fig. 2 Albedo boxplot, Normalized Differential Vegetation Index (*NDVI*), mean annual temperature, total annual precipitation, and mean annual atmospheric nitrogen deposition rate (N_{dep}) for different plant functional types (evergreen broad-leaf forests (EBF); evergreen needle-leaf forests (ENF); deciduous broad-leaf forests (DBF); deciduous needle-leaf forests (DNF); mixed-forests (MF)) in *data set two*; the box represents from the 75th percentile to the 25th percentile, and the line inside the median; upper and lower marks are the largest (smallest) observation values that are less than or equal to the upper (lower) quartile plus 1.5 the length of the interquartile range; circles outside the lower-upper mark range are outliers.

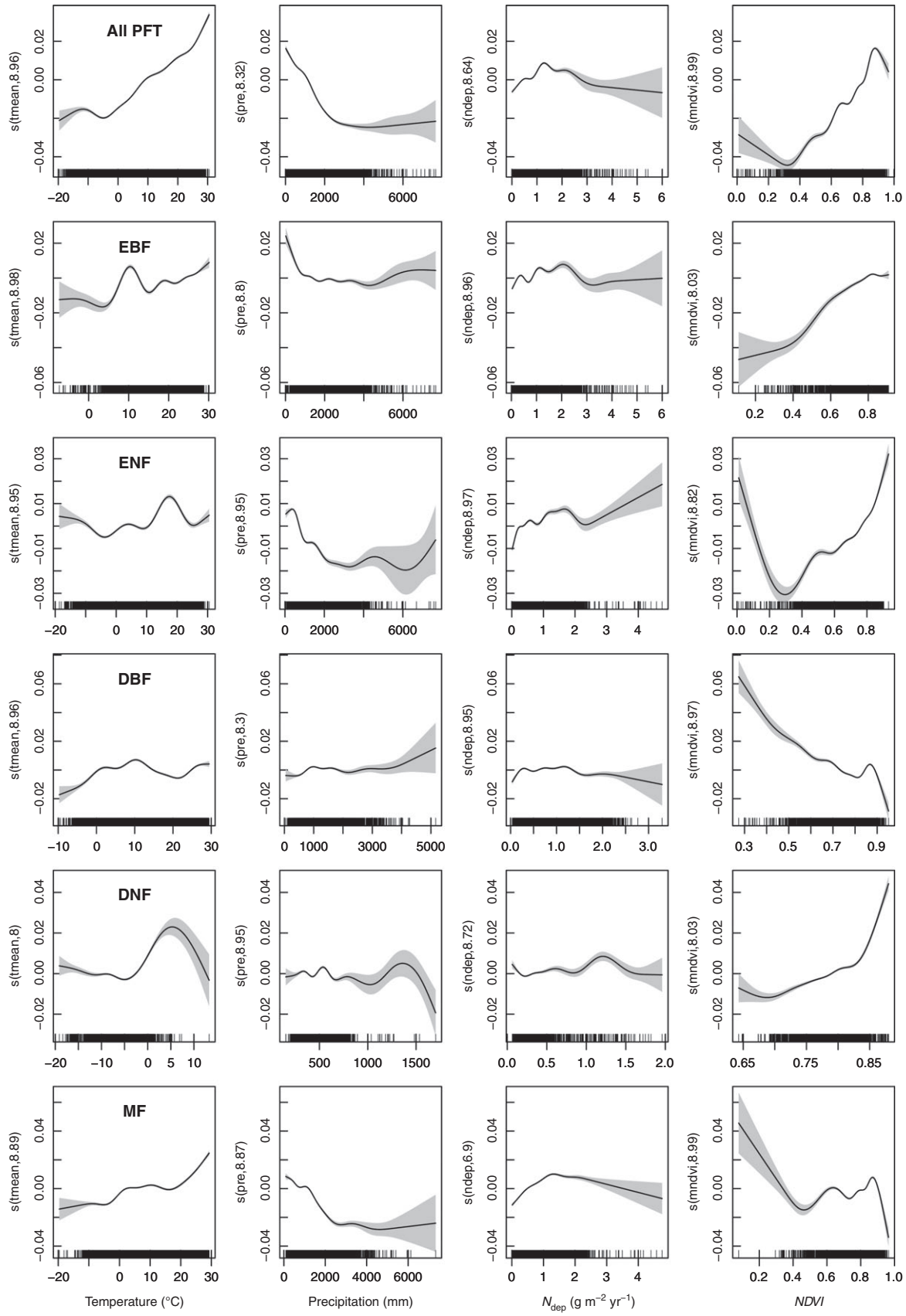
All PFT
s(tmean,8.96)
s(pre,8.32)
s(ndep,8.64)
s(mndvi,8.99)
EBF
s(tmean,8.98)
s(pre,8.8)
s(ndep,8.96)
s(mndvi,8.03)
ENF
s(tmean,8.95)
s(pre,8.95)
s(ndep,8.97)
s(mndvi,8.82)
DBF
s(tmean,8.96)
s(pre,8.3)
s(ndep,8.95)
s(mndvi,8.97)
DNF
s(tmean,8)
s(pre,8.95)
s(ndep,8.72)
s(mndvi,8.03)
MF
s(tmean,8.89)
s(pre,8.87)
s(ndep,6.9)
s(mndvi,8.99)
Temperature (°C)
Precipitation (mm)
N_{dep} (g m^{-2} yr^{-1})
NDVI

Fig. 3 *Data set one*. Generalized Additive Modeling (GAM) results of mean annual temperature, total annual precipitation, mean annual atmospheric nitrogen deposition rate (N_{dep}), and Normalized Differential Vegetation Index (*NDVI*) effects on forest surface albedo for all plant functional types pooled (All PFTs, upper panels), and for single PFTs (lower panels: evergreen broad-leaf forests (EBF); evergreen needle-leaf forests (ENF); deciduous broad-leaf forests (DBF); deciduous needle-leaf forests (DNF); mixed-forests (MF)). The continuous line is an estimate of the smooth function of the partial residuals (thus the *y*-axis is centered on zero) and indicates the *x*-axis covariate effects on the albedo deviation. The shaded areas indicate the 95% confidence interval. The number on each *y*-axis caption is the effective degrees of freedom for the term being plotted. The small lines along the *x*-axis are the 'rug', showing the observation locations.

Statistics

We used generalized additive models (*GAMs*) to explore the relationships between forest surface albedo, atmospheric nitrogen deposition rates, and climatic variables. *GAMs* are nonlinear and nonparametric regression techniques that do not require *a priori* functional relationship specifications between dependent and independent variables. The model strength is the production of link functions to define a relationship between the response variable mean and a smoothed function of each explanatory variable (Hastie & Tibshirani, 1990). As a tool for exploring single response variables, we also performed regression tree analysis (*RTA*), which implies recursive splitting the data set into increasingly homogeneous groups through repeated resampling (Breiman *et al*., 1984). All statistics were performed using the R statistical suite (R Development Core Team, 2013) using the '*mgcv*' (for *GAMs*), with default smoothing procedures, and '*rpart*' (for *RTA*) libraries.

Variability in climate and nitrogen deposition

The geographic variability of mean annual temperature, precipitation, and atmospheric nitrogen deposition for different PFT is represented as global maps in Fig. S1.

In *data set one*, large variation in climate and nitrogen deposition was apparent, among and within PFTs (Fig. 1); descriptive statistics for each variable and each PFT are reported as supplementary material (Table S1). For albedo, ENF and DNF showed notably lower values than DBF and EBF, with mixed forests (MF) exhibiting mid-range values; otherwise, variability among PFT in *NDVI* was considerably less (Fig. 1). A notable difference was apparent in mean annual temperature, again between needle-leaf (ENF and DNF) and broad-leaf (EBF and DBF) forests, with ENF and DNF shifted toward lower temperature ranges, while MF and ENF showed similar values. Again, ENF and (especially) DNF were shifted toward lower precipitation values, however, the overall variation range was reduced in this case. Atmospheric nitrogen deposition (N_{dep}) was lowest in DNF and ENF, and highest in DBF, because DBF is more concentrated at mid-latitudes, closer to the main industrialized regions.

Substantial variation in climate and nitrogen deposition remained in *data set two*, as shown by box plots (Fig. 2), and descriptive statistics (Table S2). However, it is noteworthy that although the general patterns were conserved, PFT were more differentiated than in *data set one*, particularly in precipitation and nitrogen deposition, with needle-leaf forests shifted toward lower P and N_{dep} values. Otherwise, albedo and *NDVI* variation patterns were not markedly altered (Fig. 2).

Weak correlations were found between the environmental variables, with the only exception of the correlation between T_m and P ($r = 0.68$; Fig. S2).

In agreement with global survey (e.g. Dentener *et al*., 2006), Fig. S1 shows the regions that are most affected by N_{dep} are the United States, western and eastern Europe, south and southeast Asia, and Japan. The variability among regions in nitrogen deposition has increased in recent decades (see Leonardi *et al*., 2012) and is expected to increase in the future as a consequence of different implementation of air pollution policies in different countries.

Results

Considering *data set one* and all PFTs pooled (Fig. 3, upper panels), *GAMs* show a marked positive relationship for temperature (T_m) and *NDVI* with forest surface albedo, and a marked negative relationship with precipitation (P). A positive response is evident for deposition at small values of nitrogen deposition rate (N_{dep}), which appears to level off at N_{dep} values exceeding 1 g m^{-2} yr^{-1}.

Alternatively, GAM analyses performed within single PFT data sets provides rather distinctive results, with differential response of surface albedo to environmental variables for different PFTs. If we consider GAM in regions of highest observation density (i.e. *x*-axis portions with 'thickened' lines), the most evident patterns are as follows (Fig. 3): in EBF, a less steep positive response is associated with *NDVI,* and a negative (up to 1000 mm of precipitation, approximately) response is associated with *P;* the relationship with T_m is positive, however, it is not well defined, and influenced by some over-smoothing; finally a slightly positive N_{dep} response is apparent, also obscured by possible over-smoothing effects; in needle-leaf forests (ENF), a steep positive response is again associated with *NDVI*, an evident negative response is associated with *P*, and a positive trend is apparent for N_{dep} up to a deposition rate of 2 g m^{-2} yr^{-1}; in DBF and DNF, *NDVI* is the only variable which shows a marked (negative in DBF, positive in DNF) relationship with albedo; in MF, a negative relationship is evident with *P*, and a

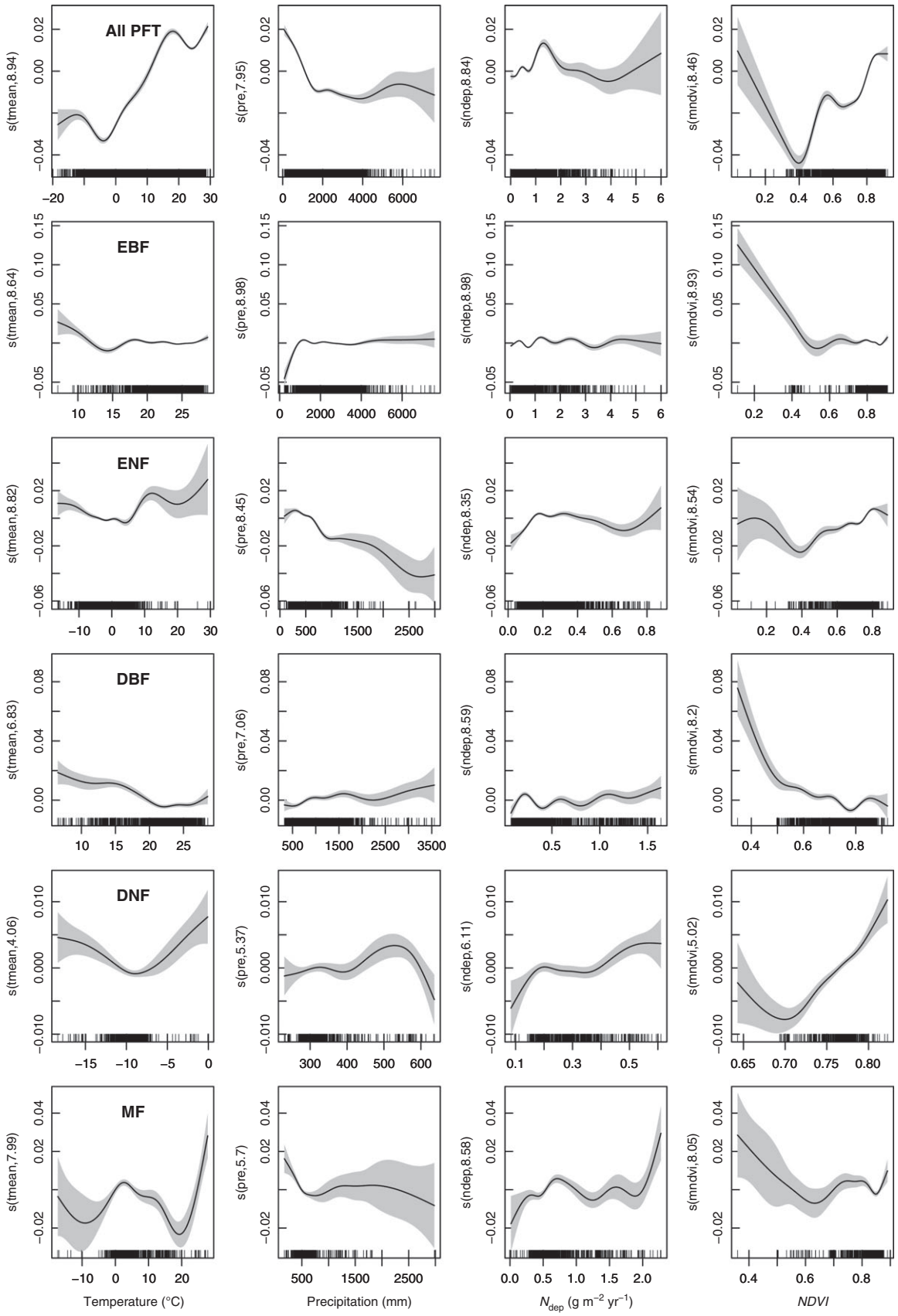
All PFT
s(tmean,8.94)
s(pre,7.95)
s(ndep,8.84)
s(mndvi,8.46)
EBF
s(tmean,8.64)
s(pre,8.98)
s(ndep,8.98)
s(mndvi,8.93)
ENF
s(tmean,8.82)
s(pre,8.45)
s(ndep,8.35)
s(mndvi,8.54)
DBF
s(tmean,6.83)
s(pre,7.06)
s(ndep,8.59)
s(mndvi,8.2)
DNF
s(tmean,4.06)
s(pre,5.37)
s(ndep,6.11)
s(mndvi,5.02)
MF
s(tmean,7.99)
s(pre,5.7)
s(ndep,8.58)
s(mndvi,8.05)
Temperature (°C)
Precipitation (mm)
N_{dep} (g m^{-2} yr^{-1})
NDVI

Fig. 4 *Data set two*. Generalized Additive Modeling (GAM) results of mean annual temperature, total annual precipitation, mean annual atmospheric nitrogen deposition rate (N_{dep}), and Normalized Differential Vegetation Index (*NDVI*) effects on forest surface albedo for all plant functional types pooled (All PFTs, upper panels), and for single PFTs (lower panels: evergreen broad-leaf forests (EBF); evergreen needle-leaf forests (ENF); deciduous broad-leaf forests (DBF); deciduous needle-leaf forests (DNF); mixed-forests (MF)). The continuous line is an estimate of the smooth function of the partial residuals (thus the *y*-axis is centered on zero) and indicates the *x*-axis covariate effects on the albedo deviation. The shaded areas indicate the 95% confidence interval. The number on each *y*-axis caption is the effective degrees of freedom for the term being plotted. The small lines along the *x*-axis are the 'rug', showing the observation locations.

positive effect with T_m and N_{dep} up to an approximate deposition rate of 1.3 g m^{-2} yr^{-1} (Fig. 3).

In the analysis performed on *data set two*, when all PFTs are pooled, *data set one* relationships are essentially confirmed. Indeed, GAMs plots show a positive relationship among forest albedo and T_m, N_{dep} (up to an ~1.5 g m^{-2} yr^{-1} deposition rate) and *NDVI*, and a negative relationship with *P*, not exceeding 2000 mm (Fig. 4). The following patterns were recognized in single PFT analyses: in EBF, only an initial positive relationship with *P* is apparent; in needle-leaf forests (ENF), a negative relationship with *P*, a positive relationship with N_{dep} (up to a 0.2 g m^{-2} yr^{-1} deposition rate), and a positive relationship with *NDVI*; in DBF, relevant patterns were not detected; in DNF, only a positive relationship with *NDVI*; and in mixed-forests (MF), interpolation patterns appeared influenced by some over-smoothing, and only a negative relationship with *P* was discernible (Fig. 4).

In all GAM analyses carried out on both data sets, the T_m, *P*, N_{dep} and *NDVI* smoothed terms were always highly significant.

In the GAM analyses described so far, space was not explicitly considered as source of variation in the model. On both data sets we also performed an analysis including the latitude × longitude as a smoothed interaction term in the GAM, and the reported relationships were confirmed in most cases (Figs S3 and S4).

Regression trees analysis performed on both data sets, using T_m, *P*, and N_{dep} as splitting variables, produced variable results (Figs S5 and S6). In several cases, T_m and *P* appear the main splitting variables, however, substantial splitting in the tree topology was also associated with N_{dep}, for example in EBF and MF (*data set one*) and EBF (*data set two*).

Discussion

Relationships across PFTs

The MODIS instrument has been providing land surface albedo estimates at regular temporal intervals (Lucht *et al*., 2000; Schaaf *et al*., 2002), and this is the first reported study to describe global-scale relationships of forest surface albedo with climatic variables and atmospheric nitrogen deposition rates (N_{dep}).

Generalized additive modeling demonstrated evident albedo patterns when data were pooled across PFTs; and environmental predictors, temperature (T_m), nitrogen deposition (N_{dep}), and *NDVI* displayed a clear positive relationship with forest albedo, while an apparent negative effect was evident for precipitation (*P*) (Fig. 3). However, all these patterns could be interpreted as the likely indirect effect of differences among different PFTs in surface albedo, primarily between conifer and broad-leaf species, and their different geographical distributions. Previous studies have shown from global-scale maps (Zhou *et al*., 2003; Moody *et al*., 2008) that surface albedo is higher in broad-leaf forests (EBF and DBF) with respect to needle-leaf forest species (ENF and DNF) (see descriptive statistics reported in Fig. 1 and Table S1 and maps in Fig. S1). In general, broad-leaf forests prevail at low latitudes, and conifer forests predominate in high latitude biomes (Loveland & Belward, 1997; Friedl *et al*., 2002; Moody *et al*., 2008), thus this underlying data structure might be responsible for much of the apparent effects of temperature and precipitation, as these variables also show a latitudinal pattern (Fig. S1). Similarly, the positive relationship with N_{dep} could be strongly affected by inherent albedo differences between deciduous broadleaves (higher albedo), which predominate in regions with high N_{dep}, and conifers (lower albedo), which tend to predominate in regions with low N_{dep} (Fig. S1). The confounding effect of varying proportions of needle-leaf and broad-leaf species, where canopy structure and surface albedo differ considerably, has recently been emphasized based on global-scale albedo variability derived from satellite data (Knyazikhin *et al*., 2012).

In this analysis, GAM patterns (Fig. 3) showed a marked increase in forest albedo with *NDVI*. As forest *NDVI* increased, a decrease in surface albedo might be expected (e.g. Melesse *et al*., 2007), as bare soil or short vegetation, which are high albedo surfaces compared to forest canopies, cover a lesser proportion of land surface; for example, a reduction in albedo was measured following bare soil or pasture afforestation (Kirschbaum *et al*., 2011). The present results showed an

inverse pattern (albedo increased with *NDVI*) when the analysis was carried out across PFTs. The positive relationship between *NDVI* and albedo was not easy to explain in the analysis. In part, it could result from an unbalanced distribution of low and high albedo forests, and also inherent uncertainties in the *NDVI-LAI* relationship (Huete *et al*., 2002; Wang *et al*., 2005), as well as different *LAI* and plant fractional cover dynamics (Block *et al*., 2011) (see below: discussion on albedo-*NDVI* relationship within PFTs).

Assessing albedo variability as a function of environmental descriptors within each individual PFT should reduce confounding effects, and related spurious effects due to differences in forest structure. Consequently, an enhanced interpretation of relationships between albedo, N_{dep}, and climate, as they emerge from GAM patterns was elucidated. Two different data sets were applied to accomplish this objective. All 0.5° spatial resolution pixels were considered, with the exception of pixel counts ≤10 in the *data set one* analysis; in the *data set two* analysis, selection of 0.5° resolution pixels was made, as described in the methods, with the aim of minimizing within-pixel variability in conifer and broad-leaf co-occurrence. Pixel number was reduced by ~80% in *data set two* with respect to *data set one*, and a smaller, albeit large, environmental variability was represented (Tables S1 and S2). Overall, we have no means to evaluate one data set as outperforming the other; therefore here we discuss the most evident albedo patterns associated with environmental predictors, as the result of GAM analysis conducted on both data sets.

In both data sets, we observed an evident short-wave albedo with *NDVI* association, but one that varied in sign between PFTs; positive in EBF, ENF, and DNF, and negative in DBF (Figs 3 and 4). *NDVI* $(R_{NIR} - R_{red})/(R_{NIR} + R_{red})$ is expected to increase with *LAI*, which determines an increase in NIR reflectance (R_{NIR}), and with plant fractional cover, which determines a decline in red reflectance (R_{red}). Short-wave albedo, on the contrary, will increase with *LAI*, but decline with increasing plant fractional cover as a result of the lower vegetation reflectance in the visible region compared to soil and litter (Block *et al*., 2011; Yao *et al*., 2011). Therefore, we could expect both positive and negative relationships between *NDVI* and albedo, depending on the relative *LAI* and plant fractional cover dynamics.

Relationships with temperature in *data set one* were detected in two forest types (MF and DNF), where a tendency for albedo to increase with temperature was clearly observed. However, straightforward ecological interpretations were difficult: in MF, an unbalanced distribution of conifer and broad-leaf species, with broad-leaf prevailing at sites with higher mean temperatures, might account for the observed pattern; in DNF, the albedo increase occurred over a very narrow temperature range (between −5 and 0 °C primarily). Moreover, these patterns largely disappeared, or were inverted, when the analysis was performed on *data set two*. This suggested that temperature *per se* can hardly be considered a key driver for forest surface albedo, and that differences in forest structure might be largely responsible for albedo variability associated with temperature.

The albedo-precipitation relationship in *data set one* showed a rather marked albedo decrease with increasing precipitation in EBF, ENF, and MF. With the exception of EBF, these patterns were well maintained when the analysis was performed on *data set two*. These relationships might result from positive precipitation effects on forest *LAI*, reported for example by Grier & Running (1977) in forest communities measured along precipitation gradients. The increase in surface albedo under low precipitation conditions might therefore reflect a reduction in forest fractional cover paralleled by an increase in higher albedo surfaces represented by shrub-graminoid vegetation, or barren soil (Kirschbaum *et al*., 2011). Overall, the negative relationship between albedo and precipitation suggested that in global evaluation of climate feedbacks involving forest changes, carbon storage reduction expected as a result of drought-induced forest tree mortality (*e.g*. Peng *et al*., 2011; Anderegg *et al*., 2012) should be considered jointly with surface albedo dynamics.

The surface albedo and atmospheric nitrogen deposition (N_{dep}) relationship in *data set one* indicated a N_{dep} effect in ENF and MF: the albedo increased with N_{dep}, and leveled at ~15 and 18 g N m^{-2} yr^{-1} in MF and ENF, respectively. In *data set two*, the relationship was only partly maintained, however, a much narrower N_{dep} range was explored.

Atmospheric nitrogen deposition might significantly affect nitrogen availability at the forest ecosystem level with related effects on carbon stock, forest growth, and canopy development, particularly in nitrogen-limited northern forest ecosystems. A positive nitrogen availability effect on tree carbon stocks was often recorded (Hyvonen *et al*., 2008; Thomas *et al*., 2010; Gentilesca *et al*., 2013), however in some cases no effects (Christ *et al*., 1995; Emmett *et al*., 1995; Magill *et al*., 2004), or even negative effects (McNulty *et al*., 1996) were observed. The effects on tree canopy cover and understory vegetation development might be variable (e.g. Siefert, 2005).

The hypothesis of a direct N_{dep} effect on forest canopy reflectance, and as a consequence, an additional role for nitrogen in the climate system via its influence on surface albedo (Ollinger *et al*., 2008), has resulted in an intense debate, summarized in the Introduction, and

now points to an effect primarily mediated by canopy architectural properties (Knyazikhin *et al*., 2012). Indeed, recent experiments on deciduous tree species, which serve to elucidate the possible mechanisms involved in the nitrogen-albedo relationship, suggest the observed increase in canopy R_{NIR}, following increased soil nitrogen availability, is mainly a consequence of changes in canopy-level characteristics, such as leaf arrangement and foliage clumping, and crown geometry (Wicklein *et al*., 2012). Ollinger (2011) indicated all these traits might depend on long-term soil nitrogen accumulation leading to enhanced plant nutritional status, therefore further research to determine possible drivers of forest canopies reflectivity has been recommended.

The following conclusions can be drawn from this study: (i) globally, the relationship between forest surface albedo, climatic variables, and atmospheric nitrogen deposition was primarily accounted for by geographic covariation in environmental variables and PFT, with higher albedo, temperature, and nitrogen deposition in broad-leaf forests; (ii) however, some relationships, *e.g*. those with annual precipitation and nitrogen deposition, were also maintained in the PFT-scale analysis. This conclusion is also supported by our attempt to select 'pure' pixels in terms of forest composition, which indicated a direct or indirect effect of environmental variables on forest surface albedo at the forest ecosystem level; and (iii) overall, our assessment emphasizes the relevance of further exploring the ecological mechanisms that link environmental conditions, forest canopy properties, and albedo, as a step to improve the parameterization of land surface albedo in climate models.

Acknowledgements

This research was supported by the MIUR-PRIN projects No. 2012E3F3LK 'Global change effects on the productivity and radiative forcing of Italian forests: a novel retrospective, experimental and prognostic analysis'. We thank Giuseppe Mancino (University of Basilicata) for the technical support.

References

Aber JD, Goodale CL, Ollinger SV *et al*. (2003) Is nitrogen deposition altering the nitrogen status of northeastern forests? *BioScience*, **53**, 375–389.

Albaugh TJ, Allen HL, Dougherty PM, Kress LW, King JS (1998) Leaf area and above- and belowground growth responses of loblolly pine to nutrient and water additions. *Forest Science*, **44**, 317–328.

Anderegg WR, Berry JA, Field CB (2012) Linking definitions, mechanisms, and modeling of drought-induced tree death. *Trends in Plant Science*, **17**, 693–700.

Barnes CA, Roy DP (2010) Radiative forcing over the conterminous United States due to contemporary land cover land use change and sensitivity to snow and interannual albedo variability. *Journal of Geophysical Research*, **115**, G04033. doi:10.1029/2010JG001428.

Betts RA (2000) Offset of the potential carbon sink from boreal forestation by decreases in surface albedo. *Nature*, **408**, 187–190.

Betts AK, Ball JH (1997) Albedo over the boreal forest. *Journal of Geophysical Research*, **102**, 28901–28928.

Block D, Schaepman-Strub G, Bartholomeus H, Heijmans MPD, Maximov TC, Berendse F (2011) The response of Arctic vegetation to the summer climate: relation between shrub cover, NDVI, surface albedo and temperature. *Environmental Research Letters*, **6**, 035502 (9pp). doi: 10.1088/1748-9326/6/3/035502.

Bobbink K, Hicks J, Spranger T *et al*. (2010) Global assessment of nitrogen deposition effects on terrestrial plant diversity: a synthesis. *Ecological Applications*, **20**, 30–59.

Bonan GB (2008) Forests and climate change: forcings, feedbacks, and the climate benefits of forests. *Science*, **320**, 1444–1449.

Breiman L, Friedman JH, Olshen RA, Stone CJ (1984) *Classification and Regression Trees*. Chapman & Hall (Wadsworth, Inc.), New York.

Cescatti A, Marcolla B, Santhana Vannan SK *et al*. (2012) Intercomparison of MODIS albedo retrievals and in situ measurements across the global FLUXNET network. *Remote Sensing of Environment*, **121**, 323–334.

Christ M, Zhang YM, Likens GE, Driscoll CT (1995) Nitrogen retention capacity of a northern hardwood forest soil under ammonium sulfate additions. *Ecological Applications*, **5**, 802–812.

Ciais P, Sabine C, Bala G *et al*. (2013) Carbon and other biogeochemical cycles. In: *Climate Change 2013: The Physical Science Basis*. Contribution of Working Group I to the Fifth Assessment Report of the Intergovernmental Panel on Climate Change (eds Stocker TF, Qin D, Plattner G-K, Tignor M, Allen SK, Boschung J, Nauels A, Xia Y, Bex V, Midgley PM), pp. 6.1.1–6.1.20. Cambridge University Press, Cambridge, UK/New York, NY.

Dail DB, Hollinger DY, Davidson EA, Fernandez I, Sievering HC, Scott NA, Gaige E (2009) Distribution of nitrogen 15-tracers applied to the canopy of a mature spruce-hemlock stand, Howland, Maine, USA. *Oecologia*, **160**, 589–599.

Dentener F, Drevet J, Lamarque JF *et al*. (2006) Nitrogen and sulfur deposition on regional and global scales: a multimodel evaluation. *Global Biogeochemical Cycles*, **20**, 1–21.

Dickinson RE (1983) Land surface processes and climate - surface albedos and energy balance. *Advances in Geophysics*, **25**, 305–353.

Emmett BA, Brittain SA, Hughes S *et al*. (1995) Nitrogen addition $NaNO_3$ and NH_4NO_3 at Aber forest, Wales: I Response of throughfall and soil water chemistry. *Forest Ecology and Management*, **71**, 45–59.

Fang H, Liang S, Kim H-Y, Townshend JR, Schaaf CL, Strahler AH, Dickinson RE (2007) Developing a spatially continuous 1 km surface albedo data set over North America from Terra MODIS products. *Journal of Geophysical Research*, **112**, D20206. doi:10.1029/2006JD008377.

Friedl MA, McIver DK, Hodges JCF *et al*. (2002) Global land cover mapping from MODIS: algorithms and early results. *Remote Sensing of Environment*, **83**, 287–302.

Gaige E, Dail DB, Hollinger DY *et al*. (2007) Changes in canopy processes following whole-forest canopy nitrogen fertilization of a mature spruce-hemlock forest. *Ecosystems*, **10**, 1133–1147.

Gallimore R, Jacob R, Kutzbach JE (2005) Coupled atmosphere- ocean-vegetation simulations for modern and mid-Holocene climates: role of extratropical vegetation cover feedbacks. *Climate Dynamics*, **25**, 755–776.

Gao F, Schaaf CB, Strahler AH, Roesch A, Lucht W, Dickinson AR (2005) MODIS bidirectional reflectance distribution function and albedo Climate Modeling Grid products and the variability of albedo for major global vegetation types. *Journal of Geophysical Research*, **110**, D01104. doi:10.1029/2004JD005190.

Gentilesca T, Vieno M, Perks MP, Borghetti M, Mencuccini M (2013) Effects of long-term nitrogen addition and atmospheric nitrogen deposition on carbon accumulation in *Picea stitchensis* plantations. *Ecosystems*, **16**, 1310–1324.

Gower ST, Vogt KA, Grier CC (1992) Carbon dynamics of Rocky Mountain Douglas-fir: influence of water and nutrient avail ability. *Ecological Monographs*, **62**, 43–65.

Grier CG, Running SW (1977) Leaf area of mature northwestern coniferous forests: relation to site water balance. *Ecology*, **58**, 893–899.

Gruber N, Galloway J (2008) An Earth-system perspective of the global nitrose cycle. *Nature*, **451**, 293–296.

Guerrieri R, Mencuccini M, Sheppard LJ *et al*. (2010) The legacy of enhanced N and S deposition as revealed by the combined analysis of $\delta^{13}C$, $\delta^{18}O$ and $\delta^{15}N$ in tree rings. *Global Change Biology*, **17**, 1946–1962.

Hastie TJ, Tibshirani RJ (1990) *Generalized Additive Models*. Chaman & Hall, New York.

Huete A, Didan K, Miura T, Rodriguez E, Gao X, Ferreira L (2002) Overview of the radiometric and biophysical performance of the MODIS vegetation indices. *Remote Sensing of Environment*, **83**, 195–213.

Hyvonen R, Persson T, Andersson S, Olsson B (2008) Impact of long-term nitrogen addition on carbon stocks in trees and soils in northern Europe. *Biogeochemistry*, **89**, 121–137.

Jin Y, Randerson JT, Goulden ML (2011) Continental-scale net radiation and evapotranspiration estimated using MODIS satellite observations. *Remote Sensing of Environment*, **115**, 2302–2319.

Kirschbaum MUF, Whitehead D, Dean SM, Beets PN, Shepherd JD, Ausseil A-GE (2011) Implications of albedo changes following afforestation on the benefits of forests as carbon sinks. *Biogeosciences*, **8**, 3687–3696.

Knyazikhin Y, Schull MA, Stenberg P *et al.* (2012) Hyperspectral remote sensing of foliar nitrogen content. *Proceedings of the National Academy of Sciences USA*, **110**, E185–E192.

Leonardi S, Gentilesca T, Guerrieri R *et al.* (2012) Assessing the effects of nitrogen deposition and climate on carbon isotope discrimination and intrinsic water-use efficiency of angiosperm and conifer trees under rising CO_2 conditions. *Global Change Biology*, **18**, 2925–2944.

Loveland TR, Belward AS (1997) The IGBP-DIS global 1-km land cover data set, DISCover: first results. *International Journal of Remote Sensing*, **65**, 1021–1031.

Lucht W, Schaaf CB, Strahler AH (2000) An algorithm for the retrieval of albedo from space using semiempirical BRDF models. *IEEE Transactions on Geoscience and Remote Sensing*, **38**, 977–998.

Magill AH, Aber JD, Currie WS *et al.* (2004) Ecosystem response to 15 years of chronic nitrogen additions at the Harward Forest LTER, Massachussets, USA. *Forest Ecology and Management*, **196**, 7–28.

Magnani F, Mencuccini M, Borghetti M *et al.* (2007) The human footprint in the carbon cycle of temperate and boreal forests. *Nature*, **447**, 848–850.

McMillan AMS, Goulden ML (2008) Age-dependent variation in the biophysical properties of boreal forests. *Global Biogeochemical Cycles*, **22**, GB2019, doi: 10.1029/2007GB003038.

McNulty SG, Aber JD, Newman SD (1996) Nitrogen saturation in a high elevation spruce-fir stand. *Forest Ecology and Management*, **84**, 109–121.

Melesse AM, Nangia V, Wang X, McClain M (2007) Wetland restoration response analysis using MODIS and groundwater data. *Sensors*, **7**, 1916–1933.

Moody EG, King MD, Schaaf CB, Platnik S (2008) MODIS-derived spatially complete surface albedo products: spatial and temporal pixel distribution and zonal averages. *Journal of Applied Meteorology & Climatology*, **47**, 2879–2894.

Myneni RB, Hall FG, Sellers PJ, Marshak AL (1995) The interpretation of spectral vegetation indexes. *IEEE Transactions on Geoscience and Remote Sensing*, **33**, 481–486.

Ollinger SV (2011) Sources of variability in canopy reflectance and the convergent properties of plants. *New Phytologist*, **189**, 375–394.

Ollinger SV, Richardson AD, Martin ME *et al.* (2008) Canopy nitrogen, carbon assimilation, and albedo in temperate and boreal forests: functional relations and potential climate feedbacks. *Proceedings of the National Academy of Sciences USA*, **105**, 19336–19341.

Peng C, Ma Z, Lei X *et al.* (2011) A drought-induced pervasive increase in tree mortality across Canada's boreal forests. *Nature Climate Change*, **1**, 467–471.

Phoenix GK, Emmett BA, Britton AJ *et al.* (2012) Impacts of atmospheric nitrogen deposition: responses of multiple plant and soil parameters across contrasting ecosystems in long-term field experiments. *Global Change Biology*, **18**, 1197–1215.

R Development Core Team (2013) *R A Language and Environment for Statistical Computing*. R Foundation for Statistical Computing, Wien, Austria. Available at: http://www.R-project.org.

Schaaf CB, Gao F, Strahleret AH *et al.* (2002) First operational BRDF, albedo nadir reflectance products from MODIS. *Remote Sensing of Environment*, **83**, 135–148.

Schlesinger WH (2009) On the fate of anthropogenic nitrogen. *Proceedings of the National Academy of Sciences USA*, **106**, 203–208.

Schultz MG, Backman L, Balkanski Y *et al.* (2007) REanalysis of the TROpospheric chemical composition over the past 40 years (RETRO) - A long-term global modeling study of tropospheric chemistry. Final Report. Jülich GmbH, Hamburg, Germany, ISSN 1614-1199.

Siefert A (2005) *Effects of Changes in Canopy Cover on Understory Vegetation in the Long Island Pine Barrens*. Pine Barrens Research Forum, Brookhaven, New York.

Sievering H, Tomaszewski T, Torizzo J (2007) Canopy uptake of atmospheric N deposition at a conifer forest. Part I - Canopy N budget, photosynthetic efficiency and net ecosystem exchange. *Tellus B*, **59**, 483–492.

Thomas RQ, Canham CD, Weathers KC, Goodale CL (2010) Increased tree carbon storage in response to nitrogen deposition in the US. *Nature Geoscience*, **3**, 13–17.

Townsend PA, Serbin SP, Kruger EL, Gamon JA (2013) Disentangling the contribution of biological and physical properties of leaves and canopies in imaging spectroscopy data. *Proceedings of the National Academy of Sciences USA*, **110**, E1074. doi:10.1073/pnas.1300952110.

Wang Q, Adiku S, Tenhunen J, Granier A (2005) On the relationship of NDVI with leaf area index in a deciduous forest site. *Remote Sensing of Environment*, **94**, 244–255.

Westoby M (1984) The self-thinning rule. *Advances in Ecological Research*, **14**, 167–225.

Wicklein HF, Ollinger SV, Martin ME *et al.* (2012) Variation in foliar nitrogen and albedo in response to nitrogen fertilization and elevated CO_2. *Oecologia*, **169**, 915–925.

Yao Y, Qin Q, Ghulam A, Liu S, Zhao S, Xu Z, Donga H (2011) Simple method to determine the Priestley-Taylor parameter for evapotranspiration estimation using Albedo-VI triangular space from MODIS data. *Journal of Applied Remote Sensing*, **5**, 053505. doi:10.1117/1.3557817.

Zaccherio MT, Finzi AC (2007) Atmospheric deposition may affect northern hardwood forest composition by altering soil nutrient supply. *Ecological Applications*, **17**, 1929–1941.

Zhou L, Dickinson RE, Tian Y *et al.* (2003) Comparison of seasonal and spatial variations of albedos from Moderate-Resolution Imaging Spectroradiometer (MODIS) and Common Land Model. *Journal of Geophysical Research*, **108**, 4488. doi:10.1029/2002JD003326.

Supporting Information

Additional Supporting Information may be found in the online version of this article:

Figure S1. Geographic variability of mean atmospheric nitrogen deposition rate (N_{dep}, g m^{-2} y^{-1}) (first page), mean annual temperature (T_m, °C) (second page), total annual precipitation (P, mm) (third page), and for different plant functional types (evergreen broad-leaf forests (EBF); evergreen needle-leaf forests (ENF); deciduous broad-leaf forests (DBF); deciduous needle-leaf forests (DNF); mixed-forests (MF).

Figure S2. Correlation scatter plot of climatic variables (mean annual temperature T_m; total annual precipitation P), and mean atmospheric nitrogen deposition (N_{dep}) in *data set one*.

Figure S3. *Data set one*. Results of GAM models including latitude × longitude interaction term.

Figure S4. *Data set two*. Results of GAM models including latitude × longitude interaction term.

Figure S5. Regression Tree Analysis results on *data set one* (see methods) based on mean annual temperature (T_m), total annual precipitation (P), and mean annual atmospheric nitrogen deposition (N_{dep}).

Figure S6. Regression Tree Analysis results on *data set two* (see methods) based on mean annual temperature (T_m), total annual precipitation (P), and mean annual atmospheric nitrogen deposition (N_{dep}).

Table S1. Data set one. Descriptive statistics.

Table S2. Data set two. Descriptive statistics.